

Interfacial phase transitions in twinning-plane superconductors

F. Clarysse and J. O. Indekeu

Laboratorium voor Vaste-Stoffysica en Magnetisme, Katholieke Universiteit Leuven, B-3001 Leuven, Belgium

(Received 15 June 2001; published 15 February 2002)

Within the framework of Ginzburg-Landau theory we study the rich variety of interfacial phase transitions in twinning-plane superconductors. We show that the phase behavior strongly depends on the transparency of the twinning plane for electrons measured by means of the coupling parameter α_{TP} . By analyzing the solutions of the Ginzburg-Landau equations in the limit of perfectly transparent twinning planes, we predict a first-order interface delocalization transition for all type-I materials. We further perform a detailed study of the other limit in which the twinning plane is opaque. The phase diagram proves to be very rich and fundamentally different from the transparent case, recovering many of the results for a system with an external surface. In particular both first-order and critical delocalization transitions are found to be possible, accompanied by a first-order depinning transition. We provide a comparison with experimental results and discuss the relevance of our findings for type-II materials.

DOI: 10.1103/PhysRevB.65.094515

PACS number(s): 74.25.Dw, 05.70.Np, 61.72.Mm, 64.60.Fr

I. INTRODUCTION

In recent years, local enhancement of superconductivity has been predicted to provide the mechanism to induce several intriguing interfacial phase transitions in type-I superconductors.¹⁻⁵ Typical phase diagrams are calculated using the Ginzburg-Landau (GL) theory in which the enhancement is accounted for by allowing the extrapolation length b to be negative. The microscopic origin of this parameter remains an unsolved problem making the experimental verification of the theoretical results nontrivial. So far, the most feasible realization of a negative extrapolation length seems to originate from the concept of twinning-plane superconductivity (TPS), a well understood phenomenon that occurs, e.g., in Sn, In, Nb, Re, and Tl.⁶ The observation of TPS has also been reported for some high- T_c superconductors, such as YBCO and HoBCO.⁷ A twinning plane (TP) is a defect plane representing the boundary between two single-crystal regions or twins and, consequently, the physics encountered in the behavior of a superconducting/normal interface near TP's is the natural analogy to grain-boundary wetting or interface depinning, a topic which has been well studied in magnetic systems.⁸⁻¹⁰

The characteristic feature of the original GL approach of TPS is the *a priori* assumption that the TP is perfectly transparent for electrons at the microscopic level which implies that the superconducting order parameter ψ is continuous at the TP.⁶ Subsequent extensions of the theory relax this assumption allowing a discontinuity in ψ .¹¹⁻¹⁴ More specifically, a second phenomenological parameter α_{TP} is introduced to describe the coupling between the twins such that, by means of α_{TP} , one can mimic the effect of microscopically tuning the TP from completely transparent to completely opaque for electrons. In this paper we present an overview of the variety of interfacial phase transitions in the two limiting cases to develop a thorough understanding of the influence of the transparency.

Earlier work⁴ has focused on the case of mixed bulk boundary conditions with the bulk normal (N) phase on one side and the bulk superconducting (SC) phase on the other

side of the TP, at bulk two-phase coexistence. This is appropriate for the study of the proper depinning transition of an interface that is initially pinned at the TP. Here we choose to settle for the configuration of equal bulk conditions, that is, we impose the bulk N phase on both sides of the TP. In so doing we are no longer restricted to the case of bulk two-phase coexistence and this allows us to establish the complete magnetic field versus temperature phase diagram for a given material. This type of diagram is accessible to experimental verification and is relevant for comparing the present results with known TPS phase diagrams.^{6,13,14}

The solutions of the GL equations strongly depend on the boundary conditions imposed at the TP itself which in turn relates to the level of transparency, i.e., the value of α_{TP} . For highly transparent planes, corresponding to the limit $\alpha_{TP} \rightarrow 0$, it is natural to consider fully symmetric profiles for the order parameter. In the opposite limit, $\alpha_{TP} \rightarrow \infty$, the TP is completely opaque for electrons and both sides are largely independent. In this case there is a wide range of possible solutions, including profiles with ψ identically zero at one side of the TP. The latter are referred to as *wall* solutions, since they are equivalent to the ones found in a type-I superconductor with an external surface or wall characterized by a negative extrapolation length b .^{1,2} Therefore we anticipate that, in the opaque limit, we will recover to a great extent the results of a wall system. This is very different from the case of complete transparency, for which drastic qualitative modifications are predicted compared to the case with a wall.

The outline of the paper is as follows. In the next section we collect the main ideas of the GL theory applied to twinning-plane superconductors. Section III covers the results for perfectly transparent TP's. We calculate in detail the phase diagrams and provide a comparison with the predicted TPS diagrams as described in Ref. 6. The fully opaque system is the subject of Sec. IV. We present a classification of the various solutions and establish their stability to derive the phase behavior. We summarize our main results and discuss the experimental relevance in Sec. V.

II. GINZBURG-LANDAU THEORY FOR TWINNING-PLANE SUPERCONDUCTORS

We consider a type-I superconductor with a TP located at $x=0$ and impose on both sides the N phase, with $\psi=0$, as the bulk condition. The GL free-energy functional has the form

$$\Gamma[\psi, \mathbf{A}] = \int_{-\infty}^{+\infty} \mathcal{G}[\psi, \mathbf{A}] dx + \Gamma_{\text{TP}}(\psi_-, \psi_+), \quad (1)$$

with the free-energy density \mathcal{G} given by

$$\begin{aligned} \mathcal{G} = & \epsilon |\psi|^2 + \frac{\beta}{2} |\psi|^4 + \frac{1}{2m} \left| \left(\frac{\hbar}{i} \nabla - 2e\mathbf{A} \right) \psi \right|^2 \\ & + \frac{[\nabla \times \mathbf{A} - \mu_0 \mathbf{H}]^2}{2\mu_0}. \end{aligned} \quad (2)$$

As usual, $\epsilon \propto T - T_c$, where T_c is the bulk critical temperature which must be distinguished from the second critical temperature in the system, $T_{c,\text{TP}}$, below which local superconductivity sets in at the TP in zero magnetic field. Since $T_{c,\text{TP}}$ was experimentally⁶ proved to be only slightly higher than T_c , the use of the GL theory is justified. Further, $\beta > 0$ is a stabilizing parameter and \mathbf{A} is the vector potential. We choose the applied magnetic field $\mathbf{H} = H\mathbf{e}_z$ parallel to the TP. Using the notation $\psi_- \equiv \psi(0^-)$ and $\psi_+ \equiv \psi(0^+)$, the local contribution Γ_{TP} in Eq. (1) reads

$$\Gamma_{\text{TP}}(\psi_-, \psi_+) = \frac{\hbar^2}{2mb} (|\psi_+|^2 + |\psi_-|^2) + \frac{\hbar^2}{2m\alpha_{\text{TP}}} |\psi_+ - \psi_-|^2. \quad (3)$$

The first term, with $b < 0$, describes the enhancement of superconductivity and was introduced by Khlyustikov and Buzdin⁶ to reproduce theoretically the observed TPS phase diagrams. The phenomenological parameter b is the extrapolation length and can be related to the temperature difference $T_c - T_{c,\text{TP}}$. In particular, $b \propto (T_{c,\text{TP}} - T_c)^{-1/2}$ [see Sec. III, Eq. (28)]. In addition, we have followed others^{4,11-14} by adding a second term in Eq. (3) to describe the coupling between the twins. In so doing, we allow the SC wave function to be discontinuous across the TP, hence in general $\psi_- \neq \psi_+$. The coupling constant α_{TP} can be expressed in terms of the Fermi velocity and either the transmission or reflection coefficient for electrons, thus fully in terms of microscopic properties.¹² We note that for $\alpha_{\text{TP}} > 0$, the phase of the wave function is continuous at the TP, while for $\alpha_{\text{TP}} < 0$ a phase jump of π can occur.¹¹ We omit the latter possibility and restrict our attention to $\alpha_{\text{TP}} > 0$. From a physical point of view it is important to recall that the wave function must be continuous on an atomic scale, while on the mesoscopic scale defined by the characteristic lengths of the superconductor (coherence length and magnetic penetration depth) the wave function may display a discontinuity.¹⁵

In what follows we assume translational invariance in the y and z directions and choose the gauge so that $\mathbf{A} = [0, A(x), 0]$. It proves to be convenient to adopt the rescaling introduced in earlier work² using the two basic length

scales of the superconductor, i.e., the zero-field coherence length ξ and the magnetic penetration depth λ defined by

$$\xi^2 = \frac{\hbar^2}{2m|\epsilon|}, \quad \lambda^2 = \frac{m\beta}{4\mu_0 e^2 |\epsilon|}. \quad (4)$$

The ratio of λ to ξ gives the GL parameter κ , with $\kappa < 1/\sqrt{2}$ for type-I materials. For temperatures $T < T_c$ or $T > T_c$ we use ξ to scale the distances but, for simplicity, retain the notation x for the dimensionless coordinate x/ξ perpendicular to the TP. For the magnetic quantities A and H we introduce the dimensionless a and h defined by

$$a = \frac{2e\lambda}{\hbar} A, \quad h = \frac{2e\lambda^2 \mu_0}{\hbar} H, \quad (5)$$

and rescale the wave function ψ according to

$$\varphi = \psi / \sqrt{|\epsilon|/\beta}. \quad (6)$$

Note that for the case $T < T_c$ the normalization of the wave function is related to the equilibrium value of the SC order parameter through $\psi_{eq} = \sqrt{|\epsilon|/\beta}$. Consequently, φ attains the value 1 in the bulk SC phase. Finally, we rescale the free energy Γ divided by the surface area S such that $\gamma = \Gamma\beta/(\epsilon^2 \xi S)$, yielding

$$\begin{aligned} \gamma[\varphi, a] = & \int_{-\infty}^{+\infty} dx \left\{ \pm \varphi^2 + \frac{\varphi^4}{2} + \dot{\varphi}^2 + \frac{a^2 \varphi^2}{\kappa^2} + (\dot{a} - h)^2 \right\} \\ & + \frac{\xi}{b} (\varphi_-^2 + \varphi_+^2) + \frac{\xi}{\alpha_{\text{TP}}} (\varphi_- - \varphi_+)^2. \end{aligned} \quad (7)$$

The \pm refers to the sign of $T - T_c$. Minimization of γ with respect to φ and a yields the well-known GL equations

$$\ddot{\varphi} = \pm \varphi + a^2 \varphi / \kappa^2 + \varphi^3 \quad (8)$$

and

$$\ddot{a} = a \varphi^2 / \kappa^2. \quad (9)$$

In addition, two coupled boundary conditions are obtained from stationarity with respect to φ_- and φ_+

$$\dot{\varphi}_- = -\frac{\xi}{b} \varphi_- + \frac{\xi}{\alpha_{\text{TP}}} (\varphi_+ - \varphi_-), \quad (10)$$

$$\dot{\varphi}_+ = \frac{\xi}{b} \varphi_+ + \frac{\xi}{\alpha_{\text{TP}}} (\varphi_+ - \varphi_-), \quad (11)$$

while the vector potential and its first derivative must be continuous at $x=0$,

$$a(x=0^-) = a(x=0^+), \quad \dot{a}(x=0^-) = \dot{a}(x=0^+). \quad (12)$$

In the subsequent sections we aim at solving the above equations for both the transparent and the opaque limit.

III. TRANSPARENT TWINNING PLANES

A. Boundary conditions and solutions

For highly transparent TP's, $\alpha_{TP} \rightarrow 0$ and we recover the original description of TPS (Ref. 6) with a continuous order parameter at the TP, thus $\varphi_+ = \varphi_-$. Consequently, it is natural to look for fully symmetric solutions for $\varphi(x)$ of the differential equation (8). In practice this is done by initially restricting ourselves to one half space, say $x > 0$. The solution in the other half space $x < 0$ can then be constructed using $\varphi(x) = \varphi(-x)$, with $\varphi(x)$ the solution for the semi-infinite system. Note that this makes the problem very similar to the one of a semi-infinite system with an external surface,^{1,2} the only difference emerging from the behavior at $x = 0$ which is manifested most clearly in the boundary condition for the vector potential. Indeed, in the presence of an external surface, stationarity of γ with respect to $a(0)$ results in $\dot{a}(0) = h$. In the present situation, however, owing to the assumed symmetry in the profile for $\varphi(x)$ the vector potential $a(x)$ will be antisymmetric with respect to x , i.e., $a(-x) = -a(x)$ and thus obeys the condition $a(0) = 0$. This follows from Eq. (9) and the fact that a symmetric and non-zero $a(x)$ is not possible because $\dot{a}(x)$ must have the same sign everywhere. The boundary conditions for the wave function reduce in this limit to

$$\dot{\varphi}_+ = -\dot{\varphi}_- = \frac{\xi}{b} \varphi_+. \quad (13)$$

In the following analysis, we will be interested in two types of solutions distinguished by their asymptotic behavior for $|x| \rightarrow \infty$. The enhancement of superconductivity near the TP will typically induce a SC sheath (with the bulk of the system prepared in the N phase) and it is precisely the thickness of this surface sheath that characterizes the solution. Clearly, if this thickness is finite superconductivity disappears for $|x| \rightarrow \infty$ and the magnetic field penetrates such that

$$\varphi(\pm\infty) = 0, \quad \dot{a}(\pm\infty) = h. \quad (14)$$

Adapting the terminology of Refs. 1,2 which follows from the analogy to wetting transitions in adsorbed fluids,¹⁶ this solution is referred to as a *partial wetting* state. We remark that this class of solutions also includes the so-called null solution without any SC phase in the system (thus describing a SC sheath with zero thickness). On the other hand, in the case of *complete wetting* the sheath can be macroscopically thick so that it fully separates the N phase from the TP. These solutions are possible only when the magnetic field equals the thermodynamic critical field H_c at which there is bulk two-phase coexistence between the N and SC phase. Instead of Eq. (14) they obey the asymptotic conditions

$$\varphi(\pm\infty) = 1, \quad a(\pm\infty) = 0. \quad (15)$$

Remarkably, the calculation of this class of solutions is very simple and analytic results can be obtained for the entire type-I regime. Indeed, the asymptotic condition for the vector potential along with the boundary condition at $x = 0$ im-

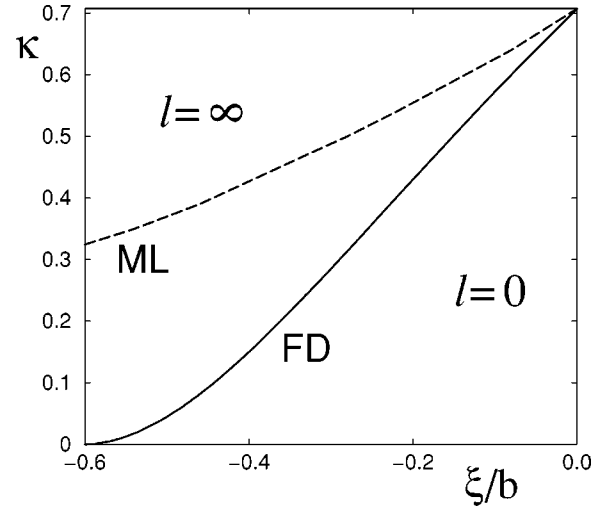


FIG. 1. Wetting phase diagram at bulk two-phase coexistence for a transparent twinning plane (TP) in the variables κ (with $0 \leq \kappa \leq 1/\sqrt{2}$) and ξ/b (with $b < 0$). The solid line represents the first-order delocalization transition and separates the region without a SC sheath ($l=0$) from that with a macroscopically thick SC layer ($l=\infty$). The dashed line is the metastability limit of the null solution corresponding to the normal state of the TP, encountered when, e.g., the temperature is increased towards T_c .

ply that $a \equiv 0$ and we are left with a single differential equation for $\varphi(x)$ taking the simplified form, for $T < T_c$,

$$\ddot{\varphi} = -\varphi + \varphi^3, \quad (16)$$

with the solution $\varphi(x) = \text{coth}[(x + \delta)/\sqrt{2}]$, for $x > 0$, and where δ is determined by the boundary condition (13).³ This solution must then be combined with a SC/N interface in the limit of $|x| \rightarrow \infty$ as necessary to obey the bulk N condition as initially imposed. This combination defines a macroscopic SC layer. For general values of κ , the SC/N interface, as well as the solutions describing a finite SC sheath, must be determined numerically. At bulk two-phase coexistence the two solutions described above may occur yielding an interface delocalization transition (or a wetting transition). This transition describes the delocalization of the SC/N interface from the TP into the bulk of the material away from the TP. We now address the analysis of this phase transition.

B. Phase diagram at bulk coexistence

In Fig. 1 we show the phase diagram for a type-I superconductor with a transparent TP as a function of the parameters κ and ξ/b . The magnetic field h is fixed to its coexistence value $h_c = 1/\sqrt{2}$.¹⁷ Varying the temperature for a given material, i.e., for fixed κ , corresponds to traveling horizontally in the diagram. Moving along coexistence towards T_c corresponds to decreasing ξ/b towards $-\infty$, since $\xi \propto |T - T_c|^{-1/2}$ and b is a negative TP constant. We distinguish two regions according to the thickness l of the SC sheath near the TP. In the first region $l=0$ indicating that the stable solution is the null solution without a SC sheath near the TP, while in the other region, the stable solution describes a macroscopic sheath on both sides of the TP and thus $l=\infty$. The free-

energy calculations and phase portrait analysis show that a solution with a strictly finite thickness, i.e. $0 < l < \infty$, always has a higher free energy than the null solution and is unstable. The two regions are separated by the equilibrium surface phase transition line FD (first-order delocalization) which marks the jump (of infinite magnitude) of the thickness of the SC surface sheath. Associated with this first-order transition is the spinodal ML (dashed line) which represents the metastability limit of the N state of the TP, when T is increased towards T_c . Hence, between FD and ML the null solution is metastable.

To identify the loci of the first-order phase boundary FD we can apply the technique of phase portraits which is a well-known concept in the study of wetting phase transitions and has proven to be equally instructive for investigating interfacial phase transitions in superconductors.^{1,2,18} In practice, however, it is simpler to calculate γ from Eq. (7) for a macroscopic SC sheath and to see where it equals the surface free energy of the null solution. Since $\gamma=0$ in the latter state the condition for the delocalization transition reads

$$\gamma_{\text{TP/SC}} + \gamma_{\text{SC/N}} = 0, \quad (17)$$

where $\gamma_{\text{TP/SC}}$ is the surface free energy of the bulk SC phase against the TP and $\gamma_{\text{SC/N}}$ the surface tension of the SC/N interface. The former can be calculated by considering the first integral of Eq.(16) (for $h=h_c$)

$$\dot{\varphi} = \frac{1}{\sqrt{2}}(1 - \varphi^2), \quad (18)$$

which leads, by inserting into the integral (7), using also Eq. (13) and considering the half space $x > 0$, to

$$\gamma_{\text{TP/SC}} = \frac{2\sqrt{2}}{3} - \varphi_+^2 \left[\frac{2\sqrt{2}}{3} \varphi_+ + \frac{\xi}{b} \right]. \quad (19)$$

Here, φ_+ is given by the solution of

$$\varphi_+^2 + \sqrt{2}\xi\varphi_+/b - 1 = 0. \quad (20)$$

This equation follows from combining the first integral with the boundary condition (13). Concerning the surface tension $\gamma_{\text{SC/N}}$ we can use the accurate analytic expression pioneered in Ref. 19 and improved in Ref. 20,

$$\gamma_{\text{SC/N}} = \frac{2\sqrt{2}}{3} - 1.02817\sqrt{\kappa} - 0.13307\kappa\sqrt{\kappa} + \mathcal{O}(\kappa^2\sqrt{\kappa}). \quad (21)$$

Due to the high accuracy of this expansion when truncated at order $\kappa\sqrt{\kappa}$ in the entire type-I regime, we immediately find, by inserting Eqs. (19) and (21) into the condition (17), an accurate analytic result for the first-order phase boundary FD. The deviation from the numerical results lies within the thickness of the solid line in Fig. 1, even at $\kappa=1/\sqrt{2}$. For $\kappa=0$ the transition occurs at $(\xi/b)^* = -0.6022$ and expanding the phase boundary about this point reveals that it approaches the $\kappa=0$ axis in a parabolic manner $\kappa(\xi/b) \sim a[\xi/b - (\xi/b)^*]^2$, with $a \approx 4.95$. This demonstrates that in

the low- κ regime the system behaves both qualitatively and quantitatively precisely like the semi-infinite system with a wall.¹⁻³

A final aspect of the phase diagram relates to the calculation of the metastability limit ML for which it is justified to use the linearized version of the GL theory. In this approximation the nonlinear terms in the GL equations are omitted so that Eq. (8) reads, for $T < T_c$,

$$\ddot{\varphi}_0 = -\varphi_0 + a_0^2\varphi_0/\kappa^2, \quad (22)$$

while the second one becomes trivial with the general solution

$$a(x) = a_0(x) = h(x + x_0), \quad (23)$$

where the boundary condition (12) immediately gives $x_0 = 0$. Eq. (23) expresses that the magnetic field is at no point expelled by the SC sheath that nucleates at ML. Thus we need only solve Eq. (22), subject to the boundary conditions

$$\dot{\varphi}_0(0^+) = \frac{\xi}{b}\varphi_0(0^+), \quad \varphi_0(\infty) = 0. \quad (24)$$

To find $\varphi_0(x)$ we follow Ref. 2 and reduce Eq. (22) to a first-order (nonlinear) differential equation by introducing the function $q_0(x) = \dot{\varphi}_0(x)/\varphi_0(x)$ obeying the equation

$$\dot{q}_0 + q_0^2 = -1 + a_0^2/\kappa^2, \quad (25)$$

with the boundary condition $q_0(0) = \xi/b$. This equation must be solved such that $q_0(x)$ has the acceptable asymptotic behavior $q_0(x) \sim -hx/\kappa$, implying a Gaussian decay for $\varphi_0(x)$. This is done by performing (backwardly) the numerical integration of the auxiliary equation

$$\dot{q}_0 + q_0^2 = -1 + (hx/\kappa)^2, \quad (26)$$

starting from $q_0(x) = -hx/\kappa$ for large x , down to $x=0$. For given h/κ , the ML value for ξ/b then simply follows from $q_0(0) = \xi/b$. Moreover, using the result for the function $q_0(x)$, we can construct explicitly a solution to Eq. (22) of the form

$$\varphi_0(x) = \varphi_0(0) \exp\left(\int_0^x q_0(x') dx'\right). \quad (27)$$

The line ML is obtained by taking a value of κ and applying the procedure for the coexistence value $h_c = 1/\sqrt{2}$. Further, the same method applies away from coexistence (as well as to $T > T_c$) where it serves to obtain the critical nucleation field as a function of temperature (see below).

The phase diagram discussed above demonstrates that for all type-I materials with an *internal transparent* TP there exists an interface delocalization transition at some temperature T_D strictly below T_c . This transition can be interpreted as a genuine wetting transition such that for temperatures $T > T_D$ the SC state completely wets the TP and this occurs on both sides of the TP. For a *transparent* TP this phase transition is of *first order* regardless of the value of κ . This is very

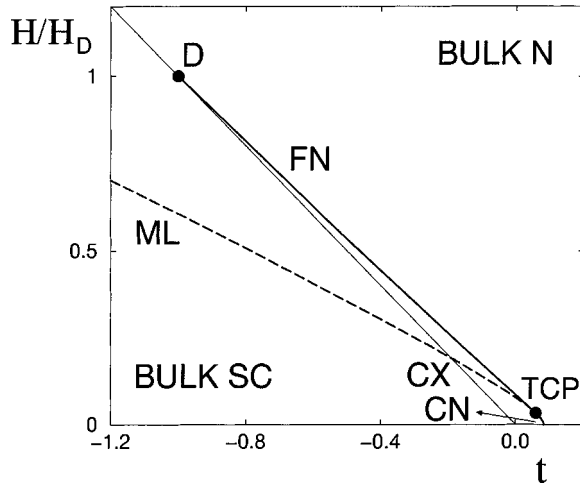


FIG. 2. Magnetic field versus temperature phase diagram for a transparent TP with $\kappa=0.3$ in the variables H/H_D and $t=(T-T_c)/(T_c-T_D)$. At the nucleation transitions FN and CN local superconductivity appears at the TP. Further details of the phase boundaries are provided in the text.

different from the analogous phase diagram for wetting at the surface of the material for which *both first-order and critical transitions* are predicted.^{1,2}

A TP displaying TPS is characterized by a negative extrapolation length, hence it is not relevant to consider here positive b values. Explicit surface free-energy calculations further reveal that for $b < 0$ the SC phase is preferred by the TP such that $\gamma_{TP/SC} < \gamma_{TP/N}$, with $\gamma_{TP/N}$ the surface free energy of the N phase in bulk, according to Eq. (14). This equality is reversed for all κ when $\xi/b > 0$ so that the question of wetting by the SC phase is only relevant for $b < 0$. In other words, the line of reversal of preferential adsorption in the $(\kappa, \xi/b)$ plane is located at $\xi/b = 0$. Also in this respect the wetting phase diagram differs from that for an external surface or wall.²

C. Off-of-coexistence phase behavior

Now we turn our attention to the issue of phenomena outside coexistence which can most easily be clarified by inspecting the magnetic field versus temperature phase diagram for a given material. These diagrams are much more accessible to experimental verification than the global diagram in Fig. 1 and provide a means of comparing our results with the TPS phase diagrams of Ref. 6.

Figure 2 shows a typical example for $\kappa=0.3$ where we employ units based on the delocalization field $H_D = H_c(T_D)$ and the delocalization temperature T_D , i.e., we take the ratios H/H_D and $t=(T-T_c)/(T_c-T_D)$. A first ingredient in this diagram is the bulk coexistence line CX at which the bulk N and SC phases are in equilibrium. On this line we identify two anchor points, the delocalization point D at $H/H_D=1$ and $t=-1$ and the bulk critical point at $H/H_D=0$ and $t=0$. Since the delocalization transition at D is first-order it has an extension into the bulk N phase region. Indeed, the point D is the starting point for a *prewetting* line

FN (first-order nucleation) which marks a first-order transition between the null solution with $l=0$ and a finite sheath. Thus, in the region confined by the lines FN and CX , the equilibrium state is a finite symmetric SC sheath, the thickness of which diverges continuously upon approach of bulk coexistence either by decreasing the field or lowering the temperature. The line FN is tangential to the coexistence line CX at D and changes into a continuous or critical nucleation line CN at a tricritical point TCP. As opposed to the first-order nucleation at which the sheath thickness jumps, at CN the sheath appears in a continuous manner. It is important to stress that this transition is critical since the sheath will appear with an infinitesimal amplitude. Concerning the spatial extension in the direction perpendicular to the TP, however, it turns out that the sheath always has a thickness of the order of ξ even just below the transition. Note that at the tricritical point FN and CN meet with common tangents and, to the left of TCP, CN continues as the metastability limit ML of the N state of the TP (dashed line). Finally, the line CN ends at zero field at the temperature $T_{c,TP}$ which obeys the equation^{1,2}

$$\frac{\xi(T_{c,TP})}{b} = -1, \quad (28)$$

showing that the extrapolation length b can be found in principle from experimental determination of $T_{c,TP}$.

We obtain the first-order nucleation line FN by numerically solving the GL equations for a sheath-type solution and finding the point in the phase diagram at which the free energy of this solution is zero. The short stretch CN can be computed using the technique discussed earlier to determine the line ML in Fig. 1. The location of TCP can be determined accurately by extending the zeroth-order solution of the linear GL equations (see above) a little further. In order to obtain a non-vanishing solution of the nonlinear theory we need a correction to $a_0(x)$ and $\varphi_0(x)$. In view of Eq. (27) $\varphi_0(x)$ is the small quantity through its small amplitude and thus it suffices to expand $a(x) = a_0(x) + a_1(x) + \dots$. Using the first integral of the equations and working to second order in φ_0 we immediately get

$$\dot{a}_1 = \frac{1}{2h} \left(\frac{a_0^2 \varphi_0^2}{\kappa^2} - \dot{\varphi}_0^2 \pm \varphi_0^2 \right), \quad (29)$$

or, using Eq. (22),

$$\dot{a}_1 = \frac{1}{2h} \dot{q}_0(x) \varphi_0^2(x). \quad (30)$$

This result is particularly useful when we use it in an alternative expression for γ evaluated in the extrema (see Ref. 2)

$$\gamma = \int_{-\infty}^{+\infty} dx \left\{ -\frac{\varphi^4}{2} + (\dot{a} - h)^2 \right\}. \quad (31)$$

The advantage of this expression is twofold, firstly the boundary term is absorbed and secondly it shows that both terms are small, of order φ_0^4 for small φ_0 . Along the line CN , $\gamma=0$ because $\varphi_0=0$ and $\dot{a}_0=h$. Another mechanism, how-

ever, to make γ vanish is the compensation of the two terms in Eq. (31), which can be put in the form

$$2h^2 = \int_{-\infty}^{+\infty} dx \dot{q}_0^2(x) \varphi_0^4(x) / \int_{-\infty}^{+\infty} dx \varphi_0^4(x), \quad (32)$$

and which is of use in determining TCP as follows. For each value of κ a continuous set of $(h, \xi/b)$ pairs can be found from the linear theory, but only one pair will satisfy the condition (32) for the onset of the nucleation of a finite (in contrast with infinitesimal) sheath, which is then by definition the TCP.

The nucleation transitions discussed above indicate the point at which local superconductivity sets in near the TP, which obviously corresponds to the phenomenon of TPS. Consequently the results presented here should agree with the predicted TPS phase diagrams for a parallel magnetic field, at least with those pertaining to strongly transparent TP's.⁶ We have checked this for various κ values and indeed found an excellent agreement for all the transitions. Furthermore, we may interpret the TPS transition as a genuine *prewetting transition* and thus by reinterpreting the existing theoretical and experimental TPS phase diagrams we stress that prewetting has since long been observed in classical superconductors. In particular the TPS transition experimentally observed by Khlyustikov and Khaikin for Sn (for a review, see Ref. 6) is fully analogous to the first-order prewetting transition which accompanies a first-order wetting phenomenon. Incidentally, we recall that only in more recent years has clear evidence of prewetting transitions been found in experiments on classical binary liquid mixtures.²¹ An important feature of the prewetting line found in superconductors is that it does not end at a surface critical point as typically predicted and found in liquid mixtures^{16,21} but becomes, via a tricritical point, a continuous nucleation line. Further, our results are particularly interesting with respect to the behavior near the wetting point D , since from the experimental TPS diagram it is unclear what happens to the TPS transition near the bulk critical field H_c . We now understand that the surface phase transition at the TP becomes a bulk transition precisely at the delocalization transition.

IV. OPAQUE TWINNING PLANES

A. Classification of solutions and terminology

In this section we focus on the second limiting case, i.e., that of completely *opaque* TP's for which $\alpha_{\text{TP}} \rightarrow \infty$. In this case the two sides of the plane are, to some extent, independent since the requirement of a continuous order parameter at $x=0$ is no longer applicable, hence for a general solution $\varphi_+ \neq \varphi_-$. However, there remains some coupling between the two half spaces due to the vector potential and the magnetic induction which must both be continuous at the TP. Moreover, the number of possible solutions is further restricted by the assumption that the extrapolation length b is equal on both sides of the TP. This means that the critical temperature $T_{c,\text{TP}}$ (which is defined for zero magnetic field) is assumed to be the same for both sides. Nevertheless, a large number of different solutions can still be found among

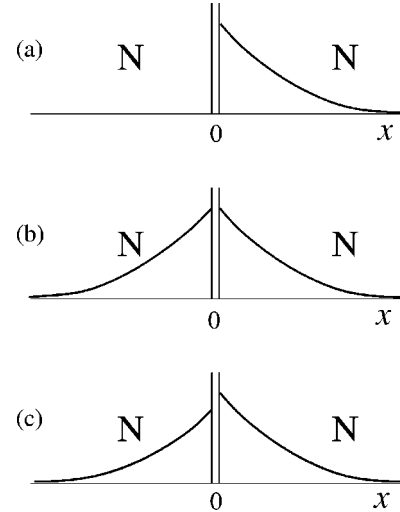


FIG. 3. Sketch of the order parameter profile for sheath-type solutions: (a) Wall solution with $\varphi(x)=0$ for $x<0$ and $\dot{a}(0)=h$. (b) Continuous solution with $\varphi_+ = \varphi_-$ and $a(0)=0$. (c) Discontinuous solution with $\varphi_+ \neq \varphi_-$ and a and \dot{a} continuous at $x=0$.

which several are characteristic for the opaque limit and deserve special attention here. For a neatly arranged description of the phases and phase transitions it is appropriate at this stage to present a classification and a schematic overview of the various solutions at bulk coexistence with equal bulk (N) conditions on the two sides of the TP.

A first (trivial) solution is the null solution $\varphi(x)=0$ without local superconductivity. For solutions with at least one finite SC sheath we distinguish three scenarios as depicted in Fig. 3. Interestingly, due to the presumed opacity we can consider imposing $\varphi(x)\equiv 0$ for one half-space, say $x<0$, leading to a solution as shown in Fig. 3(a) and referred to as “wall solution” since it corresponds exactly to the solution found in a system with a wall obeying the boundary condition $\dot{a}(0)=h$. In the case of a double SC sheath we can have either a continuous solution with $\varphi_+ = \varphi_-$ and $a(0)=0$ [Fig. 3(b)] corresponding to the sheath solution for a transparent TP, or a more general discontinuous solution with $\varphi_+ \neq \varphi_-$ and a and \dot{a} continuous at $x=0$ [Fig. 3(c)]. Arguing along the same lines we also find a series of solutions with a macroscopic SC layer on only one or on both sides of the TP. For the former, in the other half-space, we can either have the wall solution with $\varphi(x)\equiv 0$ or a finite sheath with a continuous or discontinuous order parameter at the TP. The order parameter profiles for these solutions are schematically drawn in Fig. 4. For a double macroscopic layer, on the other hand, we should in principle take into account both the continuous and discontinuous solution. It can be shown, however, by a simple argument (see below) that the latter is impossible and therefore unnecessary to consider. As outlined in the previous section a double macroscopic layer will completely expel the magnetic field such that $a=0$ over the entire region of the SC layer. Consequently expression (18) applies also here and at $x=0^{+,-}$ this yields

$$\dot{\varphi}_{+,-} = \frac{1}{\sqrt{2}}(1 - \varphi_{+,-}^2). \quad (33)$$

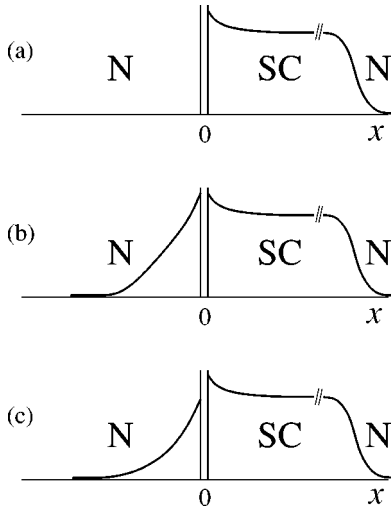


FIG. 4. Sketch of the order parameter profile for solutions with one macroscopically thick SC layer. (a) Wall solution with $\varphi(x) = 0$ for $x < 0$. (b) Continuous solution with $\varphi_+ = \varphi_-$ and a finite sheath for $x < 0$. (c) Discontinuous solution with $\varphi_+ \neq \varphi_-$ and as in (b) there is a finite sheath for $x < 0$.

While it may appear that any combination of φ_+ and φ_- obeying these equations is a possible solution, this is only true if the boundary conditions at the TP are omitted. Indeed, by applying the boundary conditions which in this case are again given by Eq. (13) it is straightforward to see that, since b is assumed to take the same value on both sides of the TP, φ_+ must equal φ_- for a solution with two macroscopic SC layers as exemplified in Fig. 5. Note that this solution is the one we found for the case of a transparent TP.

From the above classification of solutions it is obvious that an opaque TP is in a sense a combination of a system with a wall and one with a transparent TP, a feature which gives rise to additional phase transitions. Before further embarking on the phase behavior it is convenient to comment here briefly on the terminology used below. The transition from the null solution to a state with either one or two finite sheaths as well as the transition from a single sheath to a pair of sheaths is referred to as a *nucleation* phenomenon. Likewise, the transition from a “wall state” with one macroscopic SC layer to a state that is the combination of such a layer and a finite sheath is called *nucleation*. Further, the appearance of one macroscopic SC layer, either from the null solution or from one finite sheath, is a *delocalization* or *wetting transition*, while a *depinning transition* refers to the transition between one and two macroscopic layers. The latter describes the depinning of a SC/N interface that is ini-

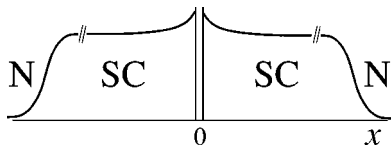


FIG. 5. Schematic order parameter profile for a continuous solution with a double macroscopic superconducting layer. Both sides of the TP are in this case wetted by the SC phase.

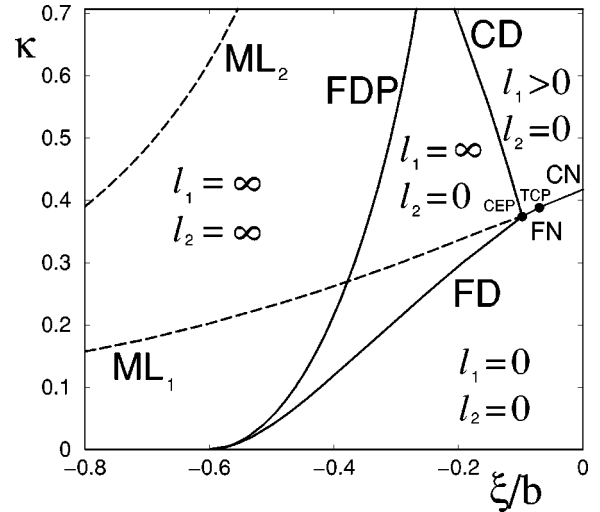


FIG. 6. Wetting phase diagram at bulk two-phase coexistence for an opaque TP in the variables κ and ξ/b . The different phases are characterized by the values l_1 and l_2 of the thicknesses of the SC sheaths on the two sides of the TP. The various transitions and transition lines are explained in the main text.

tially pinned at the TP and is analogous to the one investigated in Ref. 4. We start with a discussion of the TP states at bulk two-phase coexistence.

B. Phase diagram at bulk coexistence

The fundamental diagram for interfacial phase transitions in the case of opaque TP's is presented in Fig. 6. The different regions are distinguished according to the values of the two length scales l_1 and l_2 representing the thicknesses of the sheaths on the two sides of the TP. We assume here, without loss of generality, that $l_1 \geq l_2$. It is striking how different this phase diagram is compared to that for the case of perfect transparency, see Fig. 1. As we will demonstrate below, the main part of the diagram for the opaque case simply recovers the results of the system with a wall.¹ It is important to stress at this stage that we are only interested in the wall results for negative b values since this is the relevant region for TP's that show TPS.

One ingredient of Fig. 6 concerns the stability of the sheath solutions given in Fig. 3. From our analysis in Sec. III we know that at bulk coexistence the double symmetric sheath [Fig. 3(b)] is never stable, and hence plays no significant role. Furthermore, explicit free energy calculations reveal that the discontinuous double sheath [Fig. 3(c)] has an even higher free energy than the continuous one and thus is irrelevant. The single sheath solution [Fig. 3(a)] is stable for a certain interval of ξ/b values provided that $\kappa > 0.374$ as can be inferred from the results for a system with a wall.^{1,2} Hence, in the upper right corner of the diagram we retrieve a feature of the wall diagram, with a finite sheath on only one side of the TP while the other side is still in the N phase, thus $l_1 > 0$ and $l_2 = 0$. In the lower half of the diagram we have on the low- $|\xi/b|$ side a region where no stable sheath solution exists other than the null solution ($l_1 = 0$ and $l_2 = 0$). The two regions are separated either by the line CN (critical

nucleation) ending in a tricritical point TCP, or by the short stretch FN (first-order nucleation) between TCP and a critical end point CEP. To the left of TCP the line CN continues as the metastability limit ML_1 of the null solution.

Next we need to consider the solutions of Figs. 4 and 5 and to investigate their stability. Our calculations suggest that when the temperature is increased towards T_c the system first enters the state given in Fig. 4(a), either from one finite sheath or from the null solution. These transitions are indicated by the line CD (critical delocalization) and FD (first-order delocalization) respectively, meeting each other at the CEP. By further increasing the temperature the system undergoes a *first-order depinning transition* towards the double symmetric solution, i.e., a transition from the solution given in Fig. 4(a) towards the solution of Fig. 5. Thus the regions $l_1=\infty, l_2=0$ and $l_1=l_2=\infty$ are separated by the first-order phase boundary FDP (first-order depinning). Lastly, the line ML_2 represents the metastability limit of the state with $l_1=\infty, l_2=0$, with the SC/N interface pinned at the TP. Note that the solutions represented in Figs. 4(b) and 4(c) are never stable.

An important conclusion that we draw from this phase diagram is that for relatively low temperatures an opaque TP behaves as a system with a wall, with on one side of the TP the different wall solutions while the other side remains fully in the N phase. In other words, to the right of the line FDP in Fig. 6 we immediately obtain the phase diagram by copying the results for a wall without additional computations. All the details concerning the determination of the transition lines for this part of the diagram can be found in Refs. 2 and 3. In particular, the critical delocalization condition reads

$$\gamma_{W/N} = \gamma_{W/SC} + \gamma_{SC/N}, \quad (34)$$

while the first-order delocalization condition is simply given by

$$\gamma_{W/SC} + \gamma_{SC/N} = 0, \quad (35)$$

where $\gamma_{W/N}$ ($\gamma_{W/SC}$) is the surface free energy of the bulk N (SC) phase against a wall. The novel feature in Fig. 6 is the FDP line arising from the possibility of having a macroscopic SC layer also in the other region leading to a depinning transition at higher temperatures along with the associated spinodal ML_2 . It is precisely these two transition lines that we will be concentrating on in the remainder of this section.

The condition for the first-order depinning transition is obtained by equating the free energy of the solution with one macroscopic layer at $x>0$ and no sheath at $x<0$ to that of the solution with the double symmetric macroscopic SC layer. The former can be written conveniently as the sum $\gamma_{W/SC} + \gamma_{SC/N}$, thus the depinning condition reads

$$\gamma_{W/SC} + \gamma_{SC/N} = 2(\gamma_{TP/SC} + \gamma_{SC/N}). \quad (36)$$

In general the depinning phase boundary has to be calculated numerically. An approximate analytic result can be obtained using the powerful expansions in κ for the surface free energies. For the surface tension $\gamma_{SC/N}$ we use the result (21) while a similar expansion has been derived for $\gamma_{W/SC}$ in Ref.

3. Using these earlier results in the depinning condition (36) provides a very accurate approximation for the phase boundary across the complete type-I range with an error less than 1%. For $\kappa=0$ the depinning and the delocalization transitions coincide at $(\xi/b)^* = -0.6022$. Both phase boundaries have a parabolic foot near $\kappa=0$, i.e., $\kappa(\xi/b) \sim a(\xi/b - (\xi/b)^*)^2$ with $a \approx 27.0$ for depinning and $a \approx 4.95$ for delocalization.³ From a mathematical point of view it is interesting to examine whether the extensions of the lines FDP and CD meet in the type-II regime, for $\kappa > 1/\sqrt{2}$. The condition for a line crossing is given by combining Eqs. (34) and (36). Explicit calculations using an expansion in κ for the line CD obtained in Ref. 22 reveal indeed an intersection at $\kappa \approx 0.815$, $\xi/b \approx -0.251$.

The line ML_2 marks the nucleation of an infinitesimal sheath on one side of the TP under the condition that on the other side of the TP a macroscopic sheath is stable. To obtain this line we first compute numerically a solution for a macroscopic layer in one half space, $x>0$ say, for a given value of ξ/b subject to the condition $\dot{a}(0)=h$. To proceed we combine it with a solution of the linear GL theory applied to the region $x<0$ using the scheme introduced in Sec. III. The zeroth-order solution for the vector potential is again given by Eq. (23) with in this case x_0 determined by the value of $a(0)$ which we get from the numerical calculation in $x>0$. Finally we have to compare $q_0(x_0)$ with the given value of ξ/b and iterate the procedure such that the two become equal. This defines the critical nucleation of the sheath in the region $x<0$. The line ML_2 is now formed by applying this method for the coexistence field h_c . The procedure is equally applicable for any other field appropriate for the study of off-of-coexistence phenomena, an issue which is addressed below.

C. TPS phase diagrams

From the properties of an opaque TP at bulk coexistence elucidated above we anticipate that the onset of local superconductivity near this plane generally happens in two steps. This is a natural consequence of the stability of “wall solutions” in these systems with $\varphi(x)=0$ on one side of the TP while on the other side the SC phase has already nucleated. We now wish to concentrate on the various nucleation phenomena, the order of which depends on the parameter κ , as a function of magnetic field and temperature.

For $\kappa < 0.374$ the delocalization transition on one side of the TP is first order and thus will have a prewetting extension into the region of the phase diagram where the N phase is stable in bulk. This prewetting line FN is the first-order nucleation of a sheath on one side of the TP, and hence corresponds to the transition between the null solution and a solution as given in Fig. 3(a). This line will be tangential to the bulk coexistence line CX at the first-order delocalization point D and changes at the tricritical point TCP into a continuous nucleation line CN . The latter describes the nucleation of one infinitesimal sheath and continues as the metastability limit ML_1 of the null solution to the left of TCP. So far the surface phase diagram, an example of which is given in Fig. 7 for $\kappa=0.3$, coincides with the phase diagram for the

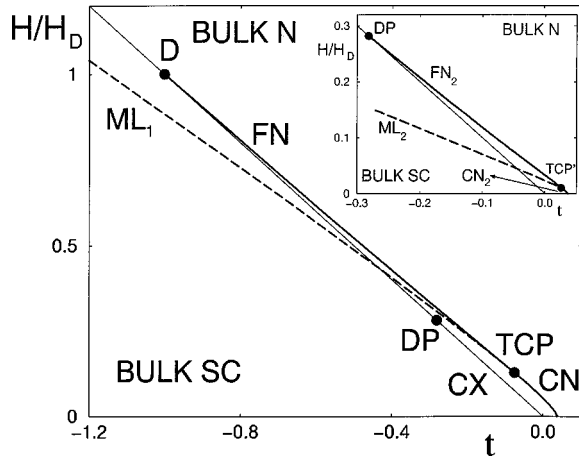


FIG. 7. Surface phase diagram for an opaque TP with $\kappa=0.3$ in the variables H/H_D and $t=(T-T_c)/(T_c-T_D)$. The inset shows the different nucleation transitions near the first-order depinning point DP. All the transitions are explained in the text.

system with a wall.^{1,2} For this reason, we do not repeat previously published details of the calculations here, but refer the interested reader to these earlier works. Note that we use the same units as in Fig. 2.

As we have argued above, however, another distinct point exists at bulk coexistence at higher temperatures but still below T_c , namely, the first-order depinning point DP , at which a double macroscopic SC layer appears. This depinning transition obviously is not present in the previous works concerned with the system with a wall, and leads to a variety of additional phase transitions. Indeed, due to the first-order character of this point a second first-order nucleation line FN_2 appears, attached to the point DP , at which the SC phase nucleates on the side of the TP where a SC sheath is not yet present. Hence it is the transition between one sheath and a double symmetric sheath. We note that this phase boundary can be interpreted as a *predepinning* line, in analogy with the prewetting line attached to the first-order delocalization transition. For the sake of clarity this line is omitted in the main figure, with all the details near the depinning transition given in the inset of Fig. 7. The line FN_2 is tangential to the line CX at DP and meets a continuous nucleation line CN_2 at a second tricritical point TCP' . To the left of TCP' , CN_2 continues as the metastability limit ML_2 of the state with one sheath. Thus, between FN_2 and ML_2 , the solution with one sheath is a metastable state, while CN_2 denotes the critical nucleation of a second SC sheath with a finite sheath already present on the other side of the TP. The two critical nucleation lines end in zero field at the same point $t_{c,TP}$ which follows from the assumption that the TP is characterized by a single value of the parameter b .

For materials with $\kappa > 0.374$ for which the delocalization transition is critical, the field-temperature phase diagram will undergo qualitative changes as regards the wettinglike transitions, i.e., the transitions related to the nucleation of the SC phase on *one* side of the TP. We refer interested readers to Ref. 2 for examples of (H, T) -phase diagrams containing these nucleation transitions and restrict ourselves here to a brief discussion of the pertinent features relevant for the

present study. For $\kappa=0.374$ the point D and the starting point of the first-order nucleation line FN separate and by further increasing κ this first-order transition disappears. The critical nucleation line CN then extends to low temperatures without intersection with the bulk coexistence line CX . Hence in this case the nucleation of the first sheath is always critical. For the nucleation of the second sheath there is still the possibility of first-order as well as second-order transitions. In fact, we know that the depinning transition is first-order for all type-I materials so that the situation that we sketched for $\kappa=0.3$ near the depinning point DP is representative for the entire type-I regime. Thus for an *opaque* TP there are always two distinct nucleation transitions, i.e., the SC phase never appears simultaneously on both sides of the TP.

V. DISCUSSION AND CONCLUDING REMARKS

In this paper we have analyzed the phase behavior of the SC/N interface near internal TP's in type-I superconductors. Our calculations reveal that the results are highly sensitive to the boundary conditions imposed at the TP, which in turn depend on the degree of transparency of the TP for electrons. For perfectly transparent TP's the order parameter is continuous such that only symmetric profiles need to be considered and at first sight the analysis resembles that of an external surface or wall. The only differences originate from the boundary condition for the vector potential and, surprisingly, this small technical modification turns out to have dramatic consequences for the order of the delocalization transition. In particular, *for a transparent TP only first-order transitions are found for the entire type-I regime* while the possibility of critical transitions that are predicted for the wall system^{1,2} are suppressed. Our results for the magnetic field versus temperature phase diagrams are in excellent agreement with earlier experimental and theoretical results obtained in the context of TPS in classical superconductors.⁶

We comment further that our approach for the *nucleation* of the SC phase near the TP equally applies to type-II materials (with $\kappa > 1/\sqrt{2}$). Specifically, we have considered the case of Nb with $\kappa \approx 1$ for which the experimental results suggest that the properties of the TP are very close to the limiting case of perfect transparency. The nucleation transition in this case is always of second-order and our results again perfectly agree with earlier work.⁶ We remark that in this case the nucleation lines are only relevant at sufficiently high fields above their intersection with the upper critical field H_{c2} .

The situation drastically changes when considering opaque TP's in which case a discontinuity in the order parameter is allowed at the TP. The decoupling of the two sides of the TP makes it possible to consider wall solutions with $\varphi(x)=0$ on one side of the TP. Moreover, from free-energy considerations, we have shown that these solutions are stable in a large region of the phase space and, as a result, the system precisely undergoes the transitions predicted for a wall system. In this case only one side of the TP will be wetted by the SC phase at the delocalization transition which can be either first-order or critical depending on the value of

κ . By further increasing the temperature at bulk coexistence a first-order depinning transition is predicted for all type-I materials. Consequently, the field-temperature phase diagrams for opaque TP's fundamentally differ from their counterparts for the transparent limit. A characteristic feature of an opaque TP is the existence of two distinct nucleation lines which in principle should be measurable and thus can *provide an experimental means of distinguishing between transparent and opaque TP's*. Related to this we remark that experiments in Sn ($\kappa \approx 0.13$) have revealed only one nucleation transition, although it is assumed that the twin boundary in this material has a low transmission for electrons.^{6,13,14} The apparent absence of a second nucleation transition can in this case be attributed to the low- κ value of the material, since in the low- κ regime the various transition lines lie extremely close together (see Fig. 6) and they would be difficult to distinguish in an experiment. Note that in the limit $\kappa \rightarrow 0$ the differences between a transparent TP, an opaque TP and an external surface vanish.

Finally, for type-II materials with opaque TP's our calculations show that the nucleation can be either first-order or critical and this is at variance with the conclusion of earlier work²³ stating that the TPS transition is always second-order for type-II materials. Our study demonstrates that this surmise is correct only for the case of transparent TP's. The reason for this is that the tricritical nucleation point TCP merges with the delocalization transition at $\kappa = 1/\sqrt{2}$ for transparent TP's. This can be seen also from the merging of the spinodal ML with the line FD in Fig. 1. In contrast, for opaque TP's the TCP of nucleation remains well off of coexistence, at $H > H_c$, and in the type-II regime at $H > H_{c2}$, so that there is room for first-order nucleation. This is further demonstrated by the fact that, in Fig. 6, the lines ML_2 and FD are still far apart at $\kappa = 1/\sqrt{2}$.

One remarkable implication of our work is that, in general, with the exception of perfectly transparent TP's, there

exist stable states of local superconductivity which are *asymmetric* about the TP. The possibility that a SC sheath or a macroscopic SC layer can occur on one side of the TP while the other side is in the normal state is indeed noteworthy and has been met with scepticism. It has been suggested that, since our analysis is essentially one dimensional and neglects states which are inhomogeneous in the direction(s) parallel to the TP, there may exist modulated states, e.g., composed of a linear array of soft vortices parallel to the TP (Ref. 14) or states with a local field penetration and a change of phase of the wave function, which may have a lower free energy than the states we have considered.²⁴ Although we cannot rule out this possibility at present, we would like to point out that asymmetric wetting, followed by symmetric depinning, has been found previously in the context of grain-boundary wetting,²⁵ in the framework of a real scalar order parameter model of Ising type.

In closing, we mention that our results are possibly relevant also to some high- T_c superconductors for which the phenomenon of enhancement of the order parameter near twinning planes was reported. Fang *et al.* measured an increase of T_c of several degrees K in macroscopic YBaCuO samples with twinning planes, and Schwartzkopf *et al.* in HoBaCuO.⁷ Abrikosov and Buzdin²⁶ also invoked the GL theory with negative extrapolation length, equivalent to $b < 0$, to describe this effect in the context of high- T_c materials.

ACKNOWLEDGMENTS

We thank Chris Boulter, Todor Mishonov and Alexander Buzdin for stimulating discussions. This research has been supported by the Belgian Fund for Scientific Research (FWO-Vlaanderen), the Inter-University Attraction Poles (IUAP) and the Concerted Action Research Program (GOA). Most of the results of this paper have been obtained in the framework of two theses (Ref. 27).

¹J.O. Indekeu and J.M.J. van Leeuwen, Phys. Rev. Lett. **75**, 1618 (1995); for a tutorial, see Physica A **236**, 114 (1997).

²J.O. Indekeu and J.M.J. van Leeuwen, Physica C **251**, 290 (1995).

³C.J. Boulter and J.O. Indekeu, Physica C **271**, 94 (1996); Int. J. Thermophys. **19**, 857 (1998).

⁴G. Backx and J.O. Indekeu, Physica C **274**, 55 (1997).

⁵E. Montecvecchi and J.O. Indekeu, Phys. Rev. B **62**, 14 359 (2000).

⁶I.N. Khlyustikov and A.I. Buzdin, Adv. Phys. **36**, 271 (1987).

⁷M.M. Fang, V.K. Kogan, D.K. Finnemore, J.R. Clem, L.S. Chumbley, and D.E. Farrell, Phys. Rev. B **37**, R2334 (1988); L.A. Schwartzkopf, M.M. Fang, L.S. Chumbley, and D.K. Finnemore, Physica C **153-155**, 1463 (1988).

⁸D.B. Abraham, in *Phase Transitions and Critical Phenomena*, edited by C. Domb and J.L. Lebowitz (Academic, London, 1986), Vol. 10.

⁹A. Sevrin and J.O. Indekeu, Phys. Rev. B **39**, 4516 (1989).

¹⁰F. Igloi and J.O. Indekeu, Phys. Rev. B **41**, 6836 (1990).

¹¹A.F. Andreev, JETP Lett. **46**, 584 (1987).

¹²V.B. Geshkenbein, Sov. Phys. JETP **67**, 2166 (1988).

¹³V.P. Mineev and K.V. Samokhin, JETP Lett. **57**, 383 (1993).

¹⁴K.V. Samokhin, JETP **78**, 909 (1994).

¹⁵P.-G. de Gennes, Rev. Mod. Phys. **36**, 225 (1964).

¹⁶For a review of wetting see, e.g., S. Dietrich, in *Phase Transitions and Critical Phenomena*, edited by C. Domb and J.L. Lebowitz (Academic, London, 1988), Vol. 12.

¹⁷This value for the thermodynamic field h_c is easily inferred from the functional for γ , Eq. (7). Indeed, the free energy density approaches in the bulk SC state the value $-1/2 + h^2$ and thus γ would diverge unless $h = h_c = 1/\sqrt{2}$.

¹⁸R. Blossey and J.O. Indekeu, Phys. Rev. B **53**, 8599 (1996).

¹⁹T.M. Mishonov, J. Phys. (France) **51**, 447 (1990).

²⁰C.J. Boulter and J.O. Indekeu, Phys. Rev. B **54**, 12 407 (1996).

²¹H. Kellay, D. Bonn, and J. Meunier, Phys. Rev. Lett. **71**, 2607 (1993); **73**, 3560 (1994).

- ²²J.M.J. van Leeuwen and E.H. Hauge, *J. Stat. Phys.* **87**, 1335 (1997).
- ²³V.V. Averin, A.I. Buzdin, and L.N. Bulaevskii, *Sov. Phys. JETP* **57**, 426 (1983).
- ²⁴A.I. Buzdin (private communication).
- ²⁵C. Ebner, F. Hayot, and J. Cai, *Phys. Rev. B* **42**, 8187 (1990).
- ²⁶A.A. Abrikosov and A.I. Buzdin, *JETP Lett.* **47**, 247 (1988).
- ²⁷F. Clarysse, B.Sc. thesis, KULeuven, 1996; Ph.D. thesis, KULeuven, 2000.